

DOI: 10.1002/adma.200602561

# Electrode Grids for ITO-free Organic Photovoltaic Devices\*\*

By Kristofer Tvingstedt and Olle Inganäs\*

The emerging field of organic photovoltaics is advancing towards commercial applications and will eventually compete with inorganic photovoltaics. Both small organic molecules and larger conjugated polymer molecules are now successfully exploited in photovoltaic devices. The conjugated polymer solar cell offers several advantages compared to their more expensive inorganic counterpart. The semiconducting polymers with extensive processing advantages, such as large area wet-printing techniques, can enable large scale and low cost production.<sup>[1]</sup> The mechanical properties of polymer materials further facilitates for coating onto flexible substrates which is a prerequisite for roll to roll manufacturing. Although the cost for inorganic photovoltaic cells slowly drops due to incremental development of production methods and economics of scale, the costs are still considered too high to compete with other (non renewable) sources of power generation. One potential alternative to the expensive cells are thin film organic photovoltaic cells.

The most efficient conjugated polymer based solar cell consists of blends of a light absorbing semiconducting polymer and a soluble derivate of the buckminster fullerene C<sub>60</sub>. The high electron affinity C<sub>60</sub> molecules provide the driving force for ultra fast charge transfer (or exciton splitting) from the photoexcited polymer. Recent polymer based bulk heterojunction solar cells show power conversion efficiency of close to 5%.<sup>[2]</sup> These cells however still lack in power conversion efficiency primarily due to too low charge carrier mobility. Furthermore, a significant limitation for cheap manufacturing on flexible substrates is the dependence on transparent conductive oxides such as Indium Tin Oxide (ITO) as charge carrier collecting electrode. The limited amount of indium available on the planet prevents large scale use of ITO in low cost photovoltaic energy conversion. Moreover, the brittleness of

conductive oxides prevents them from being operated with mechanical stability on flexible substrates.<sup>[3]</sup> Efforts have accordingly been devoted to develop highly conductive organic materials to be used in flexible organic solar cells. The so far most prominent material has been poly(3,4-ethylenedioxythiophene):poly(styrenesulphonate), PEDOT:PSS. This conductive polymer is already extensively exploited in conjunction with ITO in most organic optoelectronic devices as interfacial layer for facilitating better injection conditions. If PEDOT:PSS is processed with sorbitol, the bulk conductivity of spin coated films increases and enables working devices free of ITO as demonstrated by Zhang et al.<sup>[4]</sup> Here, the still rather limited conductivity (sheet resistance ~10<sup>3</sup> Ω/square) gives high cell series resistance and leads to significant decrease in current extraction efficiency. New forms of PEDOT:PSS with even higher conductivities are continuously being developed and investigated.<sup>[5–7]</sup>

Processing PEDOT:PSS with diethylene glycol (DEG) or a set of other inert secondary dopants leads to an enhancement of conductivity of up to 3 orders of magnitude. The exact origin of the conductivity enhancement is still under investigation but believed to come from better morphology and longer conduction paths from better interconnected PEDOT:PSS domains within the excess PSS matrix.<sup>[6,8]</sup> By including a metallic grid to further decrease the resistivity of the otherwise pure polymer anode in an organic photovoltaic cell, Aernouts et al.<sup>[9]</sup> demonstrated a threefold increase in short circuit current and hence improved cell performance. In their work, a two-sheet diffusion transfer process was exploited to deposit thick silver lines embedded in a gelatinous layer. Glatthaar et al. built inverted cells with PEDOT anode on top of the active polymer layer. Here Au lines were thermally evaporated to enhance the limited polymer conductivity.<sup>[10]</sup>

The aim of this work has been to develop a method to exclude the use of expensive ITO as transparent anode electrode in organic photovoltaic devices. The generation of metallic micro grids that does not rely on thermal evaporation through a micro structured shadow mask is a goal. Here we utilize a facile and cheap soft lithographic metal deposition method<sup>[11]</sup> in order to construct such grids to minimize the series resistance of a device with an otherwise pure polymer anode. A distributed fluidic channel system in elastomeric polydimethylsiloxane (PDMS) is filled with an electroless silvering solution to generate Ag grids of widths down to 20 μm and heights of ~100 nm, on both glass and plastic substrates. In conjunction with a highly conducting transparent polymer layer, charge carrier collection is demonstrated to be well provided for. Electroless metal deposition from such microfluidic

[\*] Prof. O. Inganäs, K. Tvingstedt  
Biomolecular and Organic Electronics  
Center of Organic Electronics (COE)  
Department of Physics, Chemistry, and Biology  
Linköping University  
58183 Linköping (Sweden)  
E-mail: ois@ifm.liu.se

[\*\*] These investigations were financially supported by the Center of Organic Electronics (COE) at Linköping University, Sweden, financed by the Strategic Research Foundation SSF. Abay Gadisa is further acknowledged for the performed impedance measurements.

channels enables easy manufacturing of charge collecting finger-like grid electrodes to be utilized in solar cell applications. The obtained photovoltaic cells display power conversion efficiencies comparable to cells with ITO. The primary effect of the metal microgrid is displayed in higher FF and photocurrent.

Patterning via photolithography has initially been exploited for the generation of the master structures in the negative photoresist SU8 (Microchem). The height of the SU8 structures ranges from 10–50  $\mu\text{m}$  depending on selected processing conditions. The resist master structures are subsequently replicated several times with polydimethylsiloxane PDMS (10:1 base:curing agent mix of Sylgard 184 from Dow Corning) and cured at 120 °C for 25 min. The cured PDMS mold is peeled off and placed in conformal contact with a glass or transparent plastic substrate. A syringe connected to a lower pressure is inserted through the PDMS mold into the closed end of the microchannels. See drawing in Figure 1.

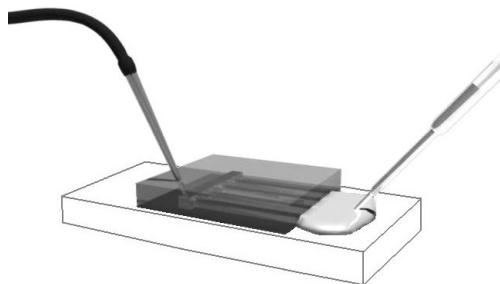


**Figure 1.** Drawing of the fluidic deposition method exploiting PDMS stamps. Air is extracted through the left syringe generating a lower pressure that speeds up the capillary flow of the deposited electroless silvering solution.

Prior to application of the stamp, the substrate is sensitized with a tin chloride sensitizer. The electroless silvering solution mixture is prepared and subsequently added at the open ends of the channels and flowed towards the other end. The driving force for the flow is a combination of capillary flow and the lower pressure originating from the syringe at the end of the channels. After flowing silvering solution for approximately 1 min, highly conductive silver stripes are formed at the sensitized bottom of the channels. The samples are then thoroughly washed in DI water and blown dried with nitrogen gas. For Ag grids to be used in small area photovoltaic applications, channel lengths of 1.5 cm were considered to be sufficient. However  $\mu$ -channels of lengths up to 5 cm have also been successfully demonstrated.

After substrates with grids are constructed and confirmed to show the expected high metal conduction they are coated with the high conductive DEG-PEDOT:PSS via spincoating. The prepared DEG-PEDOT is coated at 2000 rpm for only 10 seconds and then left to dry for about 2 min under a gentle laminar air flow. The films are then put on a hot plate and annealed at  $\sim 120^\circ$  Celsius for 1 min. This results in films with a thickness of approximately 160 nm.

Four point probe measurements are executed on reference DEG-PEDOT films deposited on pure glass in order to estimate the polymer conductivity. Sheet resistances are measured to range between 1.5 and 10  $\text{k}\Omega/\text{square}$  which corresponds to film conductivities between  $\sim 10$  and  $60 \text{ S cm}^{-1}$ . This is at its best approximately 4000 times higher than pure PEDOT:PSS films.

The generated Ag grids to be used in photovoltaic applications comprises lines with 20–40  $\mu\text{m}$  widths ( $W$ ) separated at distances ( $S$ ) of 100–800  $\mu\text{m}$  and covering areas of  $\sim 4 \text{ cm}^2$ . Figure 2A depicts optical microscope pictures of such generated grids from electroless fluidic deposition. The surface of the electroless silver grids consists of grains with diameters between 30–60 nm and is therefore generally rougher than that of a thermally evaporated metal.<sup>[12]</sup> Figure 2B and C further shows AFM scans of a section of a 40  $\mu\text{m}$  wide silver grid line. The height of the obtained silver stripes is always approximately 100 nm which results in low resistance stripes. A benefit when the Ag grid is covered with DEG-PEDOT from spincoating is that the surface becomes significantly smoother and the grid height step is lowered to  $\sim 40 \text{ nm}$ . In the manufacturing process of full solar cells this is an advantage since the roughness of the grids may otherwise create short circuits through the active layer. This risk is minimized by the smoothing of the PEDOT layer. The coverage of PEDOT on the metal striped surface was also via optical microscopy confirmed to be complete.

Four point probe measurements performed on larger areas electroless Ag films shows sheet resistances of  $\sim 0.5 \Omega/\text{square}$ . This corresponds to a conductivity of  $2 \times 10^5 \text{ S cm}^{-1}$ . Probing individual lines in the grid configuration with microprobes gives an average resistance of 86  $\Omega$  over 8 mm. With a line cross sectional area of 40  $\mu\text{m}$  to 100 nm the conductivity then equals  $2.3 \times 10^5 \text{ S cm}^{-1}$ , in good accordance with the film conductivities.

In order to design grid structures of relevant geometry and dimension a simple calculation and graphical optimization method has been performed. The best compromise between shadowing losses and resistive losses in the PEDOT layer and the Ag grid has to be found. This is a common optimization problem within ordinary inorganic semiconductor solar cell manufacturing.<sup>[13,14]</sup> The Ag grid area should be as small as possible to allow as much as possible of the impinging solar light to hit the active layer, while on the other hand the resistance of the combined PEDOT/Ag electrode should be kept as small as possible. The cell series resistance becomes large when the Ag grid is too thin and/or too widely spaced. Depending on the sheet resistance of the PEDOT layer, completely different configurations are required in optimization of the cell. As of now, a large set of PEDOT types are available with conductivities ranging from  $0.05 \text{ S cm}^{-1}$  up to  $\sim 1000 \text{ S cm}^{-1}$ .<sup>[7]</sup> Assuming a moderate value in the sheet resistance of the spin coated DEG-PEDOT film of  $10 \text{ k}\Omega/\text{square}$  and a confirmed sheet resistance of the electroless Ag of  $0.5 \Omega/\text{square}$  and plotting the total  $I^2R$  resistive fractional power losses, i.e., the sum of PEDOT fractional power losses and grid fractional

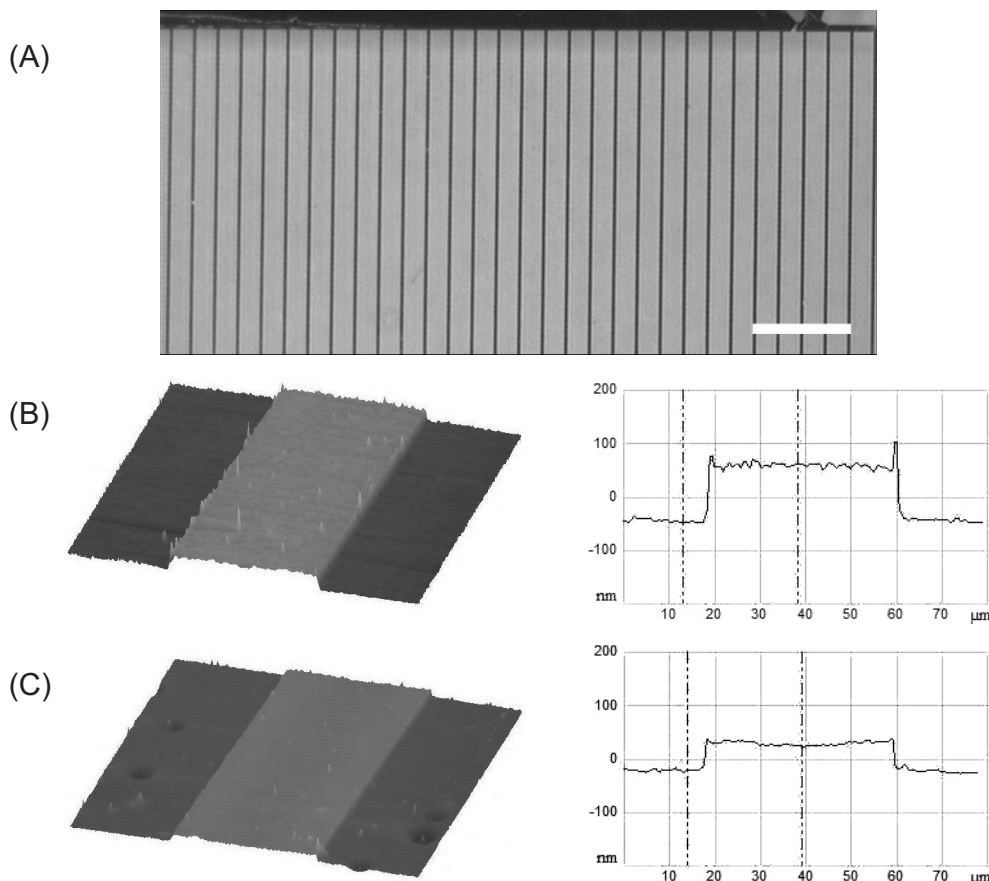


**Figure 2.** A) Optical microscope picture in transmission mode (scale bar 1 mm). AFM 3D plots and cross sectional scan of B) a single line of pure Ag grid on glass substrate and C) Ag grid covered with DEG-PEDOT on glass substrate.

power losses, versus the losses from the shadowing effect as a function of grid separation distance it is possible to obtain an optimized geometry. The shadowing fractional power losses is simply the  $W/(W+S)$  relation. The utilized optimization process is in more detail described by Cheknane et al.<sup>[14]</sup> but for the slightly different circular geometry. Figure 3 displays the calculated fractional losses as a function of grid separation. When exploiting a grid width of 40 μm it is concluded that a separation of 600 μm is close to optimal. In these simulations a minimal power loss corresponding to 6.3 % is obtained.

The transmission of the otherwise frequently used conductive oxide ITO is high in the visible part of the spectrum but less transmissive for lower energy photons. As photons from the sun with wavelengths longer than 1000 nm represents a considerable part of the total emitted solar energy there are needs for constructing low bandgap absorbers<sup>[15]</sup> that are capable of collecting this part of the solar radiation. However ITO has a limited transmission above 1000 nm and to collect these longer wavelengths alternatives for transparent electrodes are beneficial. Although PEDOT:PSS also shows lim-

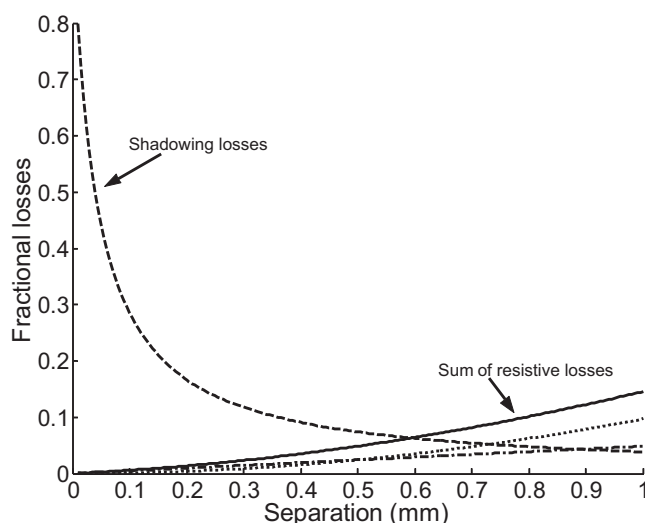


**Figure 3.** Calculations of the fractional power losses due to shadowing (dashed line) and cell electrode resistance, originating from PEDOT (dotted) and Ag lines (dash/dot), as a function of grid separation distance.

itations in transmission for longer wavelengths it is still more suited for the collection of these near infrared photons. Comparing the transmission from an ITO coated glass with an Ag  $\mu$ -grid with 40  $\mu$ m wide lines separated with a distance of 600  $\mu$ m in a Perkin Elmer  $\lambda$  950 Spectrophotometer shows that the overall transmission is comparable to that of the ITO in the visible part of the spectrum. The transmission of the grid is further confirmed to be superior in the near IR part. The light transmission in the Ag grid versus ITO is displayed in Figure 4.

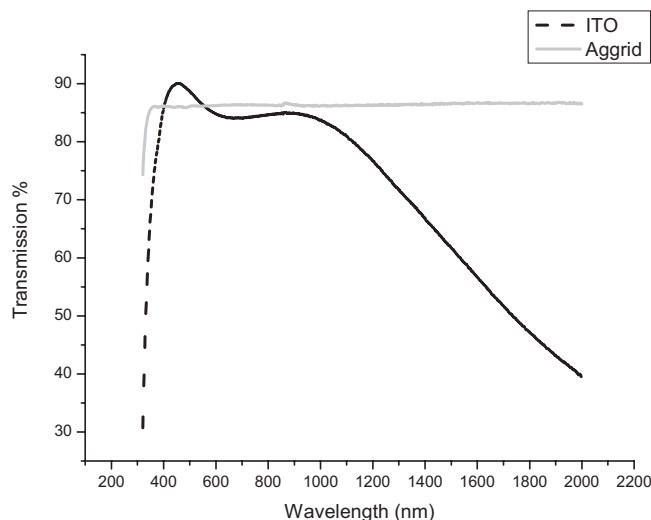


**Figure 4.** Transmission through an Ag grid on glass with line widths 40  $\mu$ m and separation 600  $\mu$ m compared to ITO on glass.

The active bulk heterojunction layer in the organic photovoltaic cell here comprise a blend of a low bandgap polyfluorene APFO-Green 5<sup>[16]</sup> as electron donor, and the methanofullerene [6,6]-phenyl C<sub>61</sub>-butyric acid methyl ester PCBM is utilized as electron acceptor molecule (chemical structures of APFO-Green 5 and PCBM are depicted in Fig. 5). For optimized devices exploiting LiF interfacial layer and ITO electrodes, power conversion efficiencies of 2.2% have been

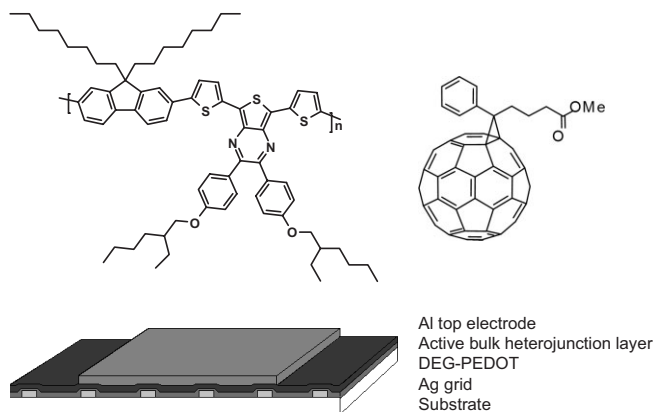


**Figure 5.** Molecular structure of APFO-Green 5 and PCBM and a schematic of the manufactured solar cell incorporating Ag grids.

obtained, and photocurrent is generated out to 800 nm.<sup>[16]</sup> The polymer and the acceptor molecules (in weight ratio of 1:3) are dissolved in chloroform and spin coated on top of the DEG-PEDOT coated Ag grid at 1000 rpm. Reference cells comprising only DEG-PEDOT anodes without Ag grids and conventional cells with ITO underneath the PEDOT layer are also manufactured. The solar cells are then finalized by depositing Al cathodes via thermal evaporation. The active areas of the constructed cells are all in the range of 8 mm<sup>2</sup>, and the thickness of the active layer is approximately 120 nm. Immediately after cathode evaporation the cells are characterized in ambient environment with a solar simulator and the relevant photovoltaic characteristics are collected. The reproducibility of the presented results is high. Although some devices are short-circuited from too rough Ag grids the yield of working devices is exceeding 80%. Representative results from these devices are presented in Figure 6 and Table 1.

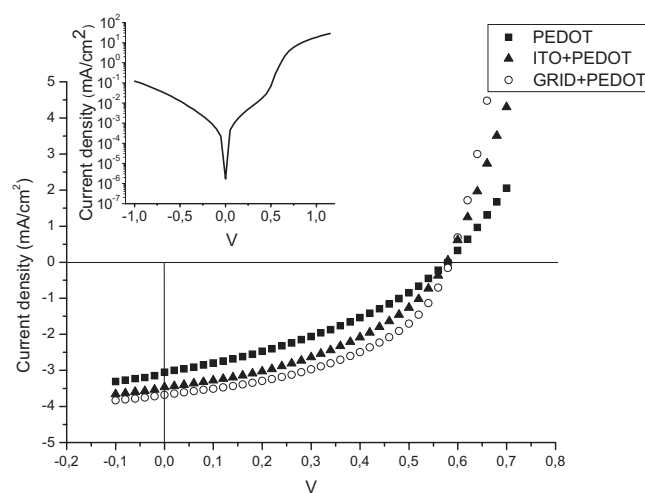


**Figure 6.** Current-voltage characteristics recorded under one sun (A.M. 1.5, 100 mW cm<sup>-2</sup>) illumination. The effect of the current collecting silver grid is primarily displayed as increased fill factor (FF) but also in short circuit current ( $J_{sc}$ ). The open circuit voltage ( $V_{oc}$ ) is to some extent governed by the work function of the electrodes but primarily governed by the difference in HOMO of the polymer donor and the LUMO of the PCBM acceptor. Hence the presence of the grids does not affect the  $V_{oc}$ . Inset: dark IV from a cell with grids.

The observed effect of the inclusion of the highly conducting Ag grid is primarily manifested in the increase of fill factor (FF) compared to devices without grid. By including geometrically optimized grids with widths of 40  $\mu$ m and separation distance of 600  $\mu$ m the FF is improved from 0.36 to 0.47. The overall power conversion efficiency is further improved from 0.63% to 1.0%. This is attributed to the significantly smaller series resistance in cells using the high conductive metal grids. To confirm this conclusion, impedance measurements have been performed on those cells manufactured with pure PEDOT anode as well as those exploiting Ag grids. The average series resistance determined from the impedance characteristics is 350  $\Omega$  for the cells with PEDOT anode and 70  $\Omega$

**Table 1.** Photovoltaic performance of cells with DEG:PEDOT anode with and without current collecting Ag grids compared to an ordinary ITO cell.

Cell exploiting:	$J_{sc}$ [mA/cm <sup>2</sup> ]	$V_{oc}$ [V]	FF	PCE [%]
PEDOT without grid	3.05	0.58	0.36	0.63
ITO with PEDOT	3.63	0.58	0.43	0.83
PEDOT with Ag grid (W=40 μm, S=600 μm)	3.67	0.58	0.47	1.00

for the ones with PEDOT/grid anodes. The presence of the highly conducting grids hence reduces the series resistance with a factor of 5. This value of 70 Ω very well equals the series resistance from a conventional cell utilizing an ITO anode. The obtained photovoltaic characteristics from cells comprising DEG-PEDOT and Ag-grids are, as seen in Table 1, very well comparable to those manufactured in the conventional way exploiting ITO. It is worth noting that the FF is actually slightly higher in the grid cell than in the ITO cell. Although devices are here manufactured primarily on solid support, small scale and on comparatively small areas no direct obstacles can be identified for up scaling to larger areas on flexible support. Larger areas may however require a different grid design geometry since the resistive losses in longer Ag grid lines will become more pronounced. The adhesion of the electroless deposited silver to sensitized plastic films is significantly stronger compared to that of evaporated metals and sputtered oxides and are hence viable for utilization in solar cells on plastics substrates.

In conclusion, this work demonstrates the possibility of excluding the expensive ITO and replace it with a set of thin conducting metal stripes that should enable printing on large flexible plastic sheets prior to use for example in roll to roll deposition of the subsequent conducting and current generating polymer layers.

## Experimental

The silvering solutions are prepared by first diluting: 300 A silvering solution, 300 B activator, and 300 C reducer (from Peacock laboratories) in 1:4 ratios with DI water. The surface sensitizer utilized was #93 Sensitizer (Peacock laboratories) that was diluted in 1:4 ratio with DI water. The three diluted silvering components (A, B, C) are then mixed under agitation in a 2:2:1 ratio. Under such mixing conditions the silvering reaction from fresh solutions is completed in 1 min after the addition of the reducer (C) component. Further dilution and less amount of the reducer agent will slow down the silvering process if required.

The high conductive DEG-PEDOT:PSS is prepared by mixing pure PEDOT:PSS (~95 %) with 5 % diethylene glycol (DEG) and 0.1 % Silquest (gamma-glycidoxypolytrimethoxysilane) and 0.1 % Zonyl FS-300 (Chemika/Fluka). The addition of the Zonyl and Silquest has the purpose of improving the wetting and adhesion to the PDMS influenced glass surface.

The *I*-*V* characteristics under simulated solar light (AM 1.5 100 mW cm<sup>-2</sup>) from a SS 50A Photo emission Tech. simulator was recorded with a Keithley 2400 source meter. The thickness of both the deposited organic films as well as the silver grids was measured by both AFM (Dimension 3100 Digital Instruments) and with a surface profilometer (Sloan Dektak). Sheet resistance was measured with an Alessi four point probe in conjunction with a Keithley 4200 semiconductor parameter analyzer. Impedance measurements were performed with an Autolab PGstat20 frequency response analyzer. All device manufacturing and characterization was executed under ambient conditions without a protective atmosphere.

Received: November 10, 2006

Revised: February 1, 2007

Published online: August 23, 2007

- [1] S.-S. Sun, N. S. Sariciftci, *Organic Photovoltaics—Mechanisms Materials and Devices*, CRC Press Taylor and Francis Group, Boca Raton, FL **2005**.
- [2] J. Y. Kim, S. H. Kim, H. H. Lee, K. Lee, W. L. Ma, X. Gong, A. J. Heeger, *Adv. Mater.* **2006**, *18*, 572.
- [3] Z. Chen, B. Cotterell, W. Wang, E. Guenther, S. J. Chua, *Thin Solid Films* **2001**, *394*, 202.
- [4] F. L. Zhang, M. Johansson, M. R. Andersson, J. C. Hummelen, O. Inganäs, *Adv. Mater.* **2002**, *14*, 662.
- [5] J. Ouyang, Q. F. Xu, C. W. Chu, Y. Yang, G. Li, J. Shinar, *Polymer* **2004**, *45*, 8443.
- [6] X. Crispin, F. L. E. Jakobsson, A. Crispin, P. C. M. Grim, P. Andersson, A. Volodin, C. van Haesendonck, M. Van der Auweraer, W. R. Salaneck, M. Berggren, *Chem. Mater.* **2006**, *18*, 4354.
- [7] B. Winther-Jensen, K. West, *Macromolecules* **2004**, *37*, 4538.
- [8] B. Y. Ouyang, C. W. Chi, F. C. Chen, Q. F. Xi, Y. Yang, *Adv. Funct. Mater.* **2005**, *15*, 203.
- [9] T. Aernouts, P. Vanlaeke, W. Geens, J. Poortmans, P. Heremans, S. Borghs, R. Mertens, R. Andriessen, L. Leenders, *Thin Solid Films* **2004**, *451–52*, 22.
- [10] M. Glatthaar, M. Niggemann, B. Zimmermann, P. Lewer, M. Riede, A. Hinsch, J. Luther, *Thin Solid Films* **2005**, *491*, 298.
- [11] E. D. Goluch, K. A. Shaikh, K. Ryu, J. Chen, J. Engel, C. Liu, *Appl. Phys. Lett.* **2004**, *85*, 3629.
- [12] Y. A. Xia, N. Venkateswaran, D. Qin, J. Tien, G. M. Whitesides, *Langmuir* **1998**, *14*, 363.
- [13] H. B. Serreze, in *13th Photovoltaic Specialist Conf.* **1978**, p. 609.
- [14] A. Cheknane, B. Benyoucef, J. P. Charles, R. Zerdoum, M. Trari, *Sol. Energy Mater. Sol. Cells* **2005**, *87*, 557.
- [15] X. J. Wang, E. Perzon, F. Oswald, F. Langa, S. Admassie, M. R. Andersson, O. Inganäs, *Adv. Funct. Mater.* **2005**, *15*, 1665.
- [16] F. Zhang, W. Mammo, L. M. Andersson, S. Admassie, M. R. Andersson, O. Inganäs, *Adv. Mater.* **2006**, *18*, 2169.